

# Impurity induced spin-orbit coupling in graphene

A. H. Castro Neto<sup>1</sup> and F. Guinea<sup>2</sup>

<sup>1</sup> *Department of Physics, Boston University, 590 Commonwealth Ave., Boston MA 02215, USA*

<sup>2</sup> *Instituto de Ciencia de Materiales de Madrid, CSIC, Cantoblanco E28049 Madrid, Spain*

We study the effect of impurities in inducing spin-orbit coupling in graphene. We show that the  $sp^3$  distortion induced by an impurity can lead to a large increase in the spin-orbit coupling with a value comparable to the one found in diamond and other zinc-blende semiconductors. The spin-flip scattering produced by the impurity leads to spin scattering lengths of the order found in recent experiments. Our results indicate that the spin-orbit coupling can be controlled via the impurity coverage.

PACS numbers: 81.05.Uw, 71.70.Ej, 71.55.Ak, 72.10.Fk

Since the discovery of graphene in 2004 [1] much has been written about its extraordinary charge transport properties [2, 3], such as sub-micron electron mean-free paths, that derive from the specificity of the carbon  $\sigma$ -bonds against atomic substitution by extrinsic atoms. However, being an open surface, it is relatively easy to hybridize the graphene's  $p_z$  orbitals with impurities with direct consequences in its transport properties [4, 5]. This capability for hybridization with external atoms, such as hydrogen (the so-called graphane), has been shown to be controllable and reversible [6] leading to new doors to control graphene's properties.

Much less has been said about the spin-related transport properties such as spin relaxation, although recent experiments show that the spin diffusion length scales [7, 8] are much shorter than what one would expect from standard spin-orbit (SO) scattering mechanisms in a  $sp^2$  bonded system [9]. In fact, atomic SO coupling in flat graphene is a very weak second order process since it affects the  $\pi$  orbitals only through virtual transitions into the deep  $\sigma$  bands [10]. Nevertheless, it would be very interesting if one could enhance SO interactions because of the prediction of the quantum spin Hall effect in the honeycomb lattice [11] and its relation to the field of topological insulators [12].

In this paper we argue that impurities (adatoms), such as hydrogen, can lead to a strong enhancement of the SO coupling due to the lattice distortions that they induce. In fact, it is well known that atoms that hybridize directly with a carbon atom induce a distortion of the graphene lattice from  $sp^2$  to  $sp^3$  [13]. By doing that, the electronic energy is lowered and the path way to chemical reaction is enhanced. Nevertheless, it has been known for quite sometime [14] that in diamond, a purely  $sp^3$  carbon bonded system, spin orbit coupling plays an important role in the band structure since it is a first order effect, of the order of the atomic SO interaction,  $\Delta_{so}^{at} \approx 10$  meV, in carbon [15]. Here we show that the impurity induced  $sp^3$  distortion of the flat graphene lattice lead to a significant enhancement of the SO coupling, explaining recent experiments [7, 8] in terms of the Elliot-Yafet mechanism for spin relaxation [16, 17] due to presence of unavoidable

environmental impurities in the experiment. Moreover, our predictions can be checked in a controllable way in graphane [6] by the control of the hydrogen coverage.

We assume that the carbon atom attached to an impurity is raised above the plane defined by its three carbon neighbors (see Fig. 1). The local orbital basis at the position of the impurity (which is assumed to be located at the origin,  $\mathbf{R}_{i=0} = 0$ ) can be written as:

$$\begin{aligned} |\pi_{i=0}\rangle &= A|s\rangle + \sqrt{1-A^2}|p_z\rangle, \\ |\sigma_{1,i=0}\rangle &= \sqrt{\frac{1-A^2}{3}}|s\rangle - \frac{A}{\sqrt{3}}|p_z\rangle + \sqrt{\frac{2}{3}}|p_x\rangle, \\ |\sigma_{2,i=0}\rangle &= \sqrt{\frac{1-A^2}{3}}|s\rangle - \frac{A}{\sqrt{3}}|p_z\rangle - \frac{1}{\sqrt{6}}|p_x\rangle + \frac{1}{\sqrt{2}}|p_y\rangle, \\ |\sigma_{3,i=0}\rangle &= \sqrt{\frac{1-A^2}{3}}|s\rangle - \frac{A}{\sqrt{3}}|p_z\rangle - \frac{1}{\sqrt{6}}|p_x\rangle - \frac{1}{\sqrt{2}}|p_y\rangle, \end{aligned} \quad (1)$$

where  $|s\rangle$ , and  $|p_{x,y,z}\rangle$ , are the local atomic orbitals. Notice that this choice of orbitals interpolates between the  $sp^2$  configuration,  $A = 0$ , to the  $sp^3$  configuration,  $A = 1/2$ . The angle  $\theta$  between the new  $\sigma$  orbitals and the direction normal to the plane is  $\cos(\theta) = -A/\sqrt{A^2+2}$ . The energy of the state  $|\pi_i\rangle$ ,  $\epsilon_\pi$ , and the energy of the three degenerate states  $|\sigma_{a,i}\rangle$ ,  $\epsilon_\sigma$  ( $a = 1, 2, 3$ ), are given by (see Fig. 2):

$$\epsilon_\pi(A) = A^2\epsilon_s + (1-A^2)\epsilon_p, \quad (2)$$

$$\epsilon_\sigma(A) = (1-A^2)\epsilon_s/3 + (2+A^2)\epsilon_p/3, \quad (3)$$

where  $\epsilon_s \approx -19.38$  eV ( $\epsilon_p \approx -11.07$  eV) is the energy of the  $s$  ( $p$ ) orbital [18]. At the impurity site one has  $A \approx 1/2$  while away from the impurity  $A = 0$ .

The Hamiltonian of the problem can be written as,  $\mathcal{H} = \mathcal{H}_\pi + \mathcal{H}_\sigma + \delta\mathcal{H}$ , where  $\mathcal{H}_\pi$  ( $\mathcal{H}_\sigma$ ) describes the  $\pi$ -band ( $\sigma$ -band) of flat graphene, and  $\delta\mathcal{H}$  describes the *local* change in the hopping energies due to the presence

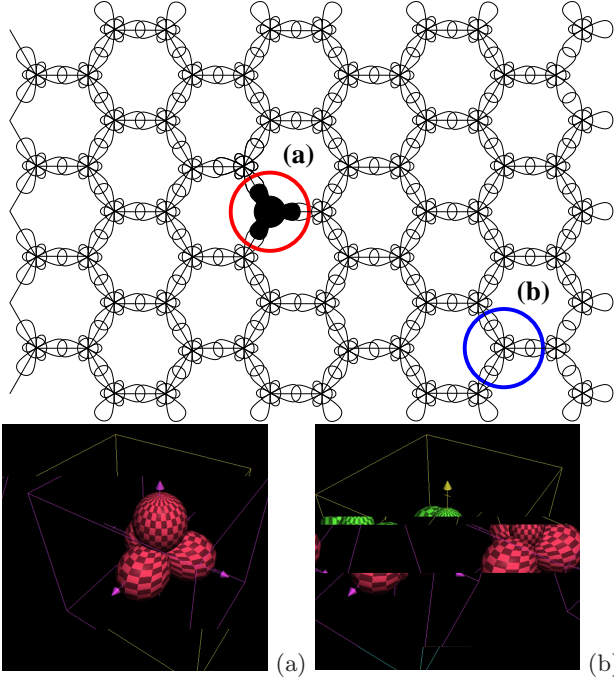


FIG. 1: (Color online). Top: Top view of the graphene lattice with its orbitals. The orbitals associated with the impurity and lattice distortion are shown in solid black. (a)  $sp^3$  orbital at impurity position; (b)  $sp^2$  orbital of the flat graphene lattice.

of the impurity and  $sp^3$  distortion:

$$\begin{aligned} \delta\mathcal{H} = & \sum_{\alpha=\uparrow,\downarrow} \left\{ \epsilon_I c_{I\alpha}^\dagger c_{I\alpha} + t_{C-I} c_{I\alpha}^\dagger c_{\pi\alpha 0} \right. \\ & + \delta\epsilon_\pi c_{\pi\alpha 0}^\dagger c_{\pi\alpha 0} + \delta\epsilon_\sigma \sum_{a=1,2,3} c_{\sigma_a\alpha 0}^\dagger c_{\sigma_a\alpha 0} \\ & \left. + V_{\pi\sigma} c_{\pi\alpha 0}^\dagger (c_{\sigma_1\alpha 0} + c_{\sigma_2\alpha 0} + c_{\sigma_3\alpha 0}) + \text{h.c.} \right\} \quad (4) \end{aligned}$$

where

$$V_{\pi\sigma}(A) = A\sqrt{\frac{1-A^2}{3}}(\epsilon_s - \epsilon_p), \quad (5)$$

$c_{I,\alpha}$  ( $c_{I,\alpha}^\dagger$ ) annihilates (creates) an electron at the impurity, and  $c_{\pi\alpha i}$  ( $c_{\sigma_a\alpha i}$ ) annihilates an electron at a carbon site in an orbital  $\pi$  ( $\sigma_a$ ) at position  $\mathbf{R}_i$  with spin  $\alpha$ ,  $\epsilon_I$  is the electron energy in the impurity, and  $t_{C-I}$  the tunneling energy between the carbon and impurity,  $\delta\epsilon_\pi(A) = \epsilon_\pi(A) - \epsilon_\pi(A=0)$ , and  $\delta\epsilon_\sigma(A) = \epsilon_\sigma(A) - \epsilon_\sigma(A=0)$ . In (4) we have not included the change in the hopping between  $\sigma_{a,0}$  orbitals (the change in energy due to the distortion is  $-A^2(\epsilon_s - \epsilon_p)/3$ ) and the inter-atomic hopping terms. In this way, we have simplified the calculations and the interpretation of the results. The inclusion of the other terms do not modify our conclusions.

The atomic spin orbit coupling,  $\mathcal{H}_{so}^{at} = \Delta_{so}^{at} \mathbf{L} \cdot \mathbf{S}$ , induces transitions between  $p$  orbitals of different spin projection [10]. In flat graphene ( $A=0$ ), it leads to transitions between the  $\pi$  and  $\sigma$  bands. The change in the

ground state energy in this case is rather small and given by:  $(\Delta_{so}^{at})^2/(\epsilon_\pi(A=0) - \epsilon_\sigma(A=0)) \approx 10^{-2}$  meV [10]. However, the perturbation described by (4) leads to a direct local hybridization  $V_{\pi\sigma}$  between the  $\pi$  and  $\sigma$  bands that modifies the effective SO coupling acting on the  $\pi$  electrons. The propagator of  $\pi$  electrons from position  $\mathbf{R}_i$  with spin  $\alpha$  to  $\mathbf{R}_j$  with spin  $\beta$  can be written as:

$$\begin{aligned} \langle \pi_{i,\alpha} | (\epsilon - \mathcal{H})^{-1} | \pi_{j,\beta} \rangle & \approx \langle \pi_{i,\alpha} | (\epsilon - \mathcal{H}_\pi)^{-1} | \pi_{0,\alpha} \rangle \\ & \times \langle \pi_{0,\alpha} | \delta\mathcal{H} | \bar{\sigma}_{0,\alpha} \rangle \times \langle \bar{\sigma}_{0,\alpha} | (\epsilon - \mathcal{H}_\sigma)^{-1} | \bar{\sigma}_{k,\alpha} \rangle \\ & \times \langle \bar{\sigma}_{k,\alpha} | \mathcal{H}_{so}^{at} | \pi_{k,\beta} \rangle \langle \pi_{k,\beta} | (\epsilon - \mathcal{H}_\pi)^{-1} | \pi_{j,\beta} \rangle \quad (6) \end{aligned}$$

where  $|\bar{\sigma}_{0,\alpha}\rangle = [|\sigma_{10,\alpha}\rangle + |\sigma_{20,\alpha}\rangle + |\sigma_{30,\alpha}\rangle]/\sqrt{3}$  and  $|\bar{\sigma}_{j,\alpha}\rangle = [|\sigma_{1j,\alpha}\rangle + e^{i\phi}|\sigma_{2j,\alpha}\rangle + e^{2i\phi}|\sigma_{3j,\alpha}\rangle]/\sqrt{3}$  where  $\phi = 2\pi/3$ . The propagator in (6) can be understood as arising from an effective non-local SO coupling within the  $\pi$  band which goes as:

$$\Delta_{so}^I(0, i) \approx V_{\pi\sigma} \langle \bar{\sigma}_{0,\alpha} | (\epsilon - \mathcal{H}_\sigma)^{-1} | \bar{\sigma}_{j,\alpha} \rangle \Delta_{so}^{at}, \quad (7)$$

which allows us to estimate the local value of the SO coupling as:

$$\frac{\Delta_{so}^I(A)}{\Delta_{so}^{at}} \approx A\sqrt{3(1-A^2)}. \quad (8)$$

As shown in Fig. 2 the value of the SO coupling depends on the angle (i.e., the value of  $A$ ) associated with the distortion of the carbon atom away from the graphene plane. Notice that for the  $sp^2$  case ( $A=0$ ) this term vanishes indicating that SO only contributes in second order in  $\Delta_{so}^{at}$ , while for the  $sp^3$  case ( $A=1/2$ ), the SO coupling is approximately 75% of the atomic value ( $\approx 7$  meV). Also observe that the dependence on the distance from the location of the hydrogen atom is determined by the Green's function  $G_\sigma(0, \mathbf{R}_j) = \langle \bar{\sigma}_0 | (\epsilon - \mathcal{H}_\sigma)^{-1} | \bar{\sigma}_j \rangle$ . This function, calculated for the simplified model of the  $\sigma$  bands discussed in ref. [10], shows a significant dispersion in Fourier space, ranging from a maximum at the  $\Gamma$  point to zero at the  $K$  and  $K'$  points. Hence, the range of  $G_\sigma(0, \mathbf{R})$  should be of the order of a few lattice constants.

Based on the previous results we can now calculate the effect of the impurity induced SO coupling in the transport properties. Firstly, we linearize the  $\pi$  band around the  $K$  and  $K'$  points in the Brillouin zone and find the 2D Dirac spectrum [3]:  $\epsilon_{\pm, \mathbf{k}} = \pm v_F k$  where  $v_F$  ( $\approx 10^6$  m/s) is the Fermi-Dirac velocity. In this long wavelength limit the impurity potential induced by (7) has cylindrical symmetry and we can use a decomposition of the wavefunction in terms of radial harmonics [19, 20, 21, 22, 23]. A similar analysis, for a system with SO interaction in the bulk has been studied in ref. [9]. We describe the potential scattering by boundary conditions such as one of the components of the spinor vanishes at a distance  $r = R_1$  (of the order of the Bohr radius) of the impurity [24]. A Rashba-like SO interaction exists in

the region  $R_1 \leq r \leq R_2$  (region I), and there is neither potential nor spin orbit interaction for  $r > R_2$ , region II ( $R_2$  if of the order of the carbon-carbon distance).

The wavefunctions in region I can be written as a superposition of angular harmonics:

$$\begin{aligned} \Psi_n(r, \theta) \equiv & A_+ \left[ \begin{pmatrix} c_+ J_n(k_+ r) e^{in\theta} \\ ic_- J_{n+1}(k_+ r) e^{i(n+1)\theta} \end{pmatrix} \left| \uparrow \right\rangle + \right. \\ & \left. + \begin{pmatrix} ic_- J_{n+1}(k_+ r) e^{i(n+1)\theta} \\ -c_+ J_{n+2}(k_+ r) e^{i(n+2)\theta} \end{pmatrix} \left| \downarrow \right\rangle \right] + \\ & + B_+ \left[ \begin{pmatrix} c_+ Y_n(k_+ r) e^{in\theta} \\ ic_- Y_{n+1}(k_+ r) e^{i(n+1)\theta} \end{pmatrix} \left| \uparrow \right\rangle + \right. \\ & \left. + \begin{pmatrix} ic_- Y_{n+1}(k_+ r) e^{i(n+1)\theta} \\ -c_+ Y_{n+2}(k_+ r) e^{i(n+2)\theta} \end{pmatrix} \left| \downarrow \right\rangle \right] + \\ & + A_- \left[ \begin{pmatrix} c'_+ J_n(k_- r) e^{in\theta} \\ ic'_- J_{n+1}(k_- r) e^{i(n+1)\theta} \end{pmatrix} \left| \uparrow \right\rangle - \right. \\ & \left. - \begin{pmatrix} ic'_+ J_{n+1}(k_- r) e^{i(n+1)\theta} \\ -c'_- J_{n+2}(k_- r) e^{i(n+2)\theta} \end{pmatrix} \left| \downarrow \right\rangle \right] + \\ & + B_- \left[ \begin{pmatrix} c'_+ Y_n(k_- r) e^{in\theta} \\ ic'_- Y_{n+1}(k_- r) e^{i(n+1)\theta} \end{pmatrix} \left| \uparrow \right\rangle - \right. \\ & \left. - \begin{pmatrix} ic'_+ Y_{n+1}(k_- r) e^{i(n+1)\theta} \\ -c'_- Y_{n+2}(k_- r) e^{i(n+2)\theta} \end{pmatrix} \left| \downarrow \right\rangle \right] \quad (9) \end{aligned}$$

where  $|\uparrow\rangle$  and  $|\downarrow\rangle$  are the spin states. The functions

$J_n(x), Y_n(x)$  are Bessel functions of order  $n$ , and:

$$\epsilon = \pm \Delta_{so}^I/2 + \sqrt{v_F^2 k_{\pm}^2 + (\Delta_{so}^I/2)^2} \quad (10)$$

$$c_{\pm} = \sqrt{1/2 \pm \Delta_{so}^I / (4\sqrt{v_F^2 k_{\pm}^2 + (\Delta_{so}^I/2)^2})} \quad (11)$$

$$c'_{\pm} = \sqrt{1/2 \pm \Delta_{so}^I / (4\sqrt{v_F^2 k_{\pm}^2 + (\Delta_{so}^I/2)^2})} \quad (12)$$

$\epsilon$  is the energy of the scattered electron ( $k_{\pm}$  is defined through (10)).

The wavefunctions outside the region affected by the impurity,  $r > R_2$ , can be written as:

$$\begin{aligned} \Psi_n(r, \theta) \equiv & \begin{pmatrix} J_n(kr) e^{in\theta} \\ iJ_{n+1}(kr) e^{i(n+1)\theta} \end{pmatrix} \left| \uparrow \right\rangle + \\ & + C_{\uparrow} \begin{pmatrix} Y_n(kr) e^{in\theta} \\ iY_{n+1}(kr) e^{i(n+1)\theta} \end{pmatrix} \left| \uparrow \right\rangle + \\ & + C_{\downarrow} \begin{pmatrix} Y_{n+1}(kr) e^{i(n+1)\theta} \\ iY_{n+2}(kr) e^{i(n+2)\theta} \end{pmatrix} \left| \downarrow \right\rangle \quad (13) \end{aligned}$$

and:  $\epsilon = v_F k$ . The boundary conditions at  $r = R_1$  and  $r = R_2$  lead to the equations:

$$\begin{aligned} c_+ A_+ J_n(k_+ R_1) + c_+ B_+ Y_n(k_+ R_1) + c'_- A_- J_n(k_- R_1) + c'_- B_- Y_n(k_- R_1) &= 0 \\ c_- A_+ J_{n+1}(k_+ R_1) + c_- B_+ Y_{n+1}(k_+ R_1) + c'_+ A_- J_{n+1}(k_- R_1) + c'_+ B_- Y_{n+1}(k_- R_1) &= 0 \\ c_+ A_+ J_n(k_+ R_2) + c_+ B_+ Y_n(k_+ R_2) + c'_- A_- J_n(k_- R_2) + c'_- B_- Y_n(k_- R_2) &= J_n(k R_2) + C_{\uparrow} Y_n(k R_2) \\ c_- A_+ J_{n+1}(k_+ R_2) + c_- B_+ Y_{n+1}(k_+ R_2) + c'_+ A_- J_{n+1}(k_- R_2) + c'_+ B_- Y_{n+1}(k_- R_2) &= J_{n+1}(k R_2) + C_{\uparrow} Y_{n+1}(k R_2) \\ c_- A_+ J_{n+1}(k_+ R_2) + c_- B_+ Y_{n+1}(k_+ R_2) - c'_+ A_- J_{n+1}(k_- R_2) - c'_+ B_- Y_{n+1}(k_- R_2) &= C_{\downarrow} Y_{n+1}(k R_2) \\ c_+ A_+ J_{n+2}(k_+ R_2) + c_+ B_+ Y_{n+2}(k_+ R_2) - c'_- A_- J_{n+2}(k_- R_2) - c'_- B_- Y_{n+2}(k_- R_2) &= C_{\downarrow} Y_{n+2}(k R_2) \quad (14) \end{aligned}$$

These six equations allow us to obtain the coefficients  $A_{\pm}, B_{\pm}, C_{\uparrow}$  and  $C_{\downarrow}$ . In the absence of the SO interaction, we have  $A_+ = A_-, B_+ = B_-, C_{\downarrow} = 0$  and  $C_{\uparrow} = -J_n(k R_1)/Y_n(k R_1)$ .

We show in Fig. 3 the results for the cross section for spin flip processes, determined by  $|C_{\downarrow}|^2/k_F$ . The main contribution arises from the  $n = 0$  channel. For comparison, the elastic cross section, calculated in the same way, is  $\sigma_{el} \approx k_F^{-1}$ . This is about three of magnitude larger than the spin-flip cross section due to the spin orbit coupling. Hence, the spin relaxation length is  $10^3$  times the elastic mean free path [9]. We obtain a mean free path of about  $1 \mu m$ , in reasonable agreement with the experimental results in ref. [7]. This value depends quadratically on  $\Delta_{so}^I(A)$ . For a finite, but small, concentration

of impurities, our results scale with the impurity concentration and hence the spin flip processes should increase roughly linearly with impurity coverage in transport experiments in systems like graphene [6].

In summary, we have shown that the impurity induced, lattice driven, SO coupling in graphene can be of the order of the atomic spin orbit coupling and comparable to what is found in diamond and zinc-blend semiconductors. The value of the SO coupling depends on how much the carbon atom which is hybridized with the impurity displaces from the plane inducing a  $sp^3$  hybridization. We have calculated the spin-flip cross section due to SO coupling for the impurity and shown that it agrees with recent experiments. This results indicates that there are substantial amounts of hybridized impu-

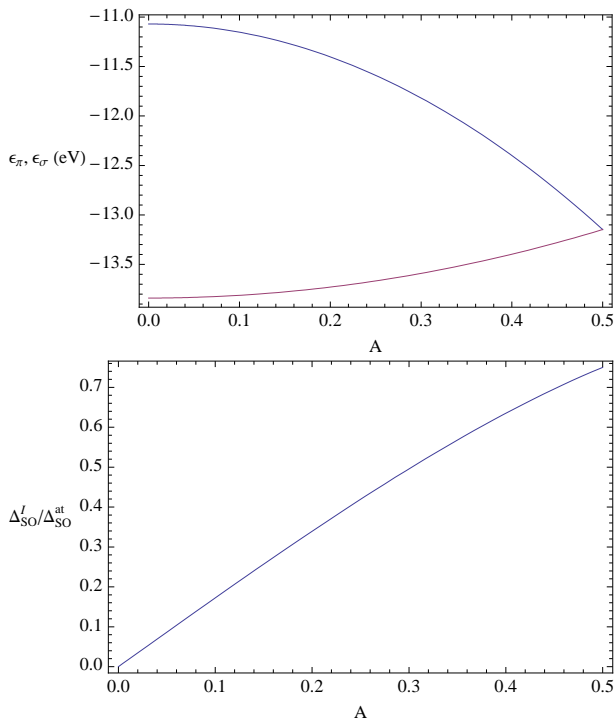


FIG. 2: (Color online). Top: Energy (in eV) of the  $\pi$  (blue) and  $\sigma$  (red) bands as a function of  $A$  according to (3); Bottom: Relative value of the SO coupling at the impurity site relative to the atomic value in carbon as a function of  $A$  according to (8).

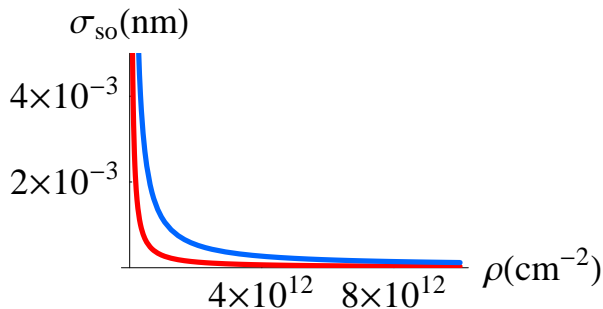


FIG. 3: (Color online). Cross section for a spin flip process for a defect as described in the text. The parameters used are  $R_1 = 1 \text{ \AA}$   $R_2 = 2 \text{ \AA}$  and  $\Delta_{so}^I = 1 \text{ meV}$  (blue) and  $\Delta_{so}^I = 2 \text{ meV}$  (red).

rities in graphene, even under ultra-clean high vacuum

conditions. Experiments where the impurity coverage is well controlled can provide a “smoking-gun” test of our predictions.

We thank illuminating discussions with D. Huertas-Hernando and A. Brataas. AHCN acknowledges the partial support of the U.S. Department of Energy under grant DE-FG02-08ER46512. FG acknowledges support from MEC (Spain) through grant FIS2005-05478-C02-01 and CONSOLIDER CSD2007-00010, by the Comunidad de Madrid, through CITECNOMIK, CM2006-S-0505-ESP-0337.

- 
- [1] K. S. Novoselov *et al.*, *Science* **306**, 666 (2004).
  - [2] A. K. Geim and K. S. Novoselov, *Nature Materials* **6**, 183 (2007).
  - [3] A. H. Castro Neto *et al.*, *Rev. Mod. Phys.* **81**, 109 (2009).
  - [4] J. H. Chen *et al.*, *Nat. Phys.* **4**, 377 (2008).
  - [5] P. Blake *et al.* (2008), arXiv:0810.4706.
  - [6] D. C. Elias *et al.*, *Science* **323**, 610 (2009).
  - [7] N. Tombros *et al.*, *Nature* **448**, 571 (2007).
  - [8] N. Tombros *et al.*, *Phys. Rev. Lett.* **101**, 046601 (2008).
  - [9] D. Huertas-Hernando, F. Guinea, and A. Brataas (2008), arXiv:0812.1921.
  - [10] D. Huertas-Hernando, F. Guinea, and A. Brataas, *Phys. Rev. B* **74**, 155426 (2006).
  - [11] C. L. Kane and E. J. Mele, *Phys. Rev. Lett.* **95**, 226801 (2005).
  - [12] C. Kane and E. Mele, *Science* **314**, 1692 (2006).
  - [13] E. J. Duplock, M. Scheffler, and P. J. Lindan, *Phys. Rev. Lett.* **92**, 225502 (2004).
  - [14] P. Y. Yu and M. Cardona, *Fundamentals of Semiconductors: Physics and Materials Properties* (Springer, New York, 2005).
  - [15] J. Serrano, M. Cardona, and T. Ruf, *Solid St. Commun.* **113**, 411 (2000).
  - [16] P. G. Elliot, *Phys. Rev.* **96**, 266 (1954).
  - [17] Y. Yafet, in *Solid State Physics, vol 13*, edited by ed. by F. Seitz and D. Turnbull (Academic, New York, 1963).
  - [18] W. A. Harrison, *Solid State Theory* (Dover, New York, 1980).
  - [19] P. M. Ostrovsky, I. V. Gornyi, and A. D. Mirlin, *Phys. Rev. B* **74**, 235443 (2006).
  - [20] M. Hentschel and F. Guinea, *Phys. Rev. B* **76**, 115407 (2007).
  - [21] D. S. Novikov, *Phys. Rev. B* **76**, 245435 (2007).
  - [22] M. I. Katsnelson and K. S. Novoselov, *Solid State Commun.* **143**, 3 (2007).
  - [23] F. Guinea, *Journ. Low Temp. Phys.* **153**, 359 (2008).
  - [24] V. M. Pereira *et al.*, *Phys. Rev. Lett.* **96**, 036801 (2006).